Research article

Comprehensive mapping of Neurofibromin 1 (NF1) expression in developing mouse brain

Vishal Lolam[1] and Achira Roy[1,*]

[1]Neurodevelopment Laboratory, Neuroscience Unit, Jawaharlal Nehru Centre for Advanced Scientific Research (JNCASR), India

***Correspondence:** Achira Roy, MSc, PhD
Assistant Professor
Neurodevelopment Lab, Room: SBS-B201, Neuroscience Unit,
Jawaharlal Nehru Centre for Advanced Scientific Research (JNCASR),
Rachenahalli Lake Road, Jakkur PO, Bangalore, India. PIN: 560064
achira.roy@jncasr.ac.in

Short Title: NF1 expression in mouse brain

Keywords: NF1, antibody, brain expression, cerebellum, single-cell reanalysis

Total number of words: 4094

Number of Figures: 9
Number of Supplementary Figures: 3

Abstract:

Neurofibromin 1 (NF1) is a critical negative regulator of the RAS-RAF-ERK pathway, mutations in which have been clinically implicated in various neurodevelopmental disorders. However, the lack of a high-resolution spatiotemporal map has obscured the understanding of why specific cell populations and developmental processes are uniquely vulnerable to *NF1* loss. In this study, we present a comprehensive atlas of NF1 expression in the developing mouse brain. Using *in situ* hybridization and immunohistochemistry, we characterized NF1 distribution from early embryonic stages through postnatal maturation. We further integrated these findings with single-nuclei RNA-sequencing (snRNA-seq) datasets from adult mouse brain to achieve higher resolution. Our results reveal a previously undocumented graded expression pattern of NF1 across various brain regions and lineages. This comprehensive study will not only help in understanding the fundamental role of NF1 during brain development but will also be pivotal in providing a framework to study *NF1*-associated brain disorders.

Introduction:

Neurofibromatosis type 1 is one of the most common autosomal dominant neurogenetic disorders, affecting approximately 1 in 3,000 individuals worldwide (Nix et al. 2020). The condition is caused by mutations in the *NF1* gene, which encodes neurofibromin, a large multifunctional protein that serves as a critical negative regulator of the RAS-RAF-ERK pathway (Karaconji et al. 2019). NF1 consists of the RAS-GTPase activating (GAP) domain, which facilitates the conversion of RAS-GTP (Active) to RAS-GDP (inactive), thereby acting as a negative regulator of RAS (Martin et al. 1990). Since the RAS-RAF-ERK pathway is important for cell growth, proliferation and survival, NF1 acts as a brake on cellular growth and proliferation (Cichowski & Jacks 2001). In case of Neurofibromatosis type 1 patients, this brake is lost, resulting in the formation of benign or malignant tumours in the brain and brain stem (Albers & Gutmann 2009; Lucas et al. 2022; Ayasa et al. 2024). Interestingly, a significant proportion of these pediatric patients develop neurodevelopmental disorders such as cortical malformations, epilepsy, hydrocephalus, autism spectrum disorder, intellectual disability and movement disorders (Balestri et al. 2003; Sorrentino et al. 2021; Roth et al. 2019; Plasschaert et al. 2015; Hyman et al. 2005; Rietman et al. 2017; Lolam & Roy 2025). These clinical findings suggest the importance of NF1 in neurodevelopment beyond its canonical role in tumorigenesis.

Despite the profound impact of *NF1* mutations on central nervous system (CNS) function, our understanding of the spatio-temporal dynamics of *NF1* expression during brain development remains incomplete. Previous studies have established that NF1 is essential for embryonic development, with null mice dying in utero between embryonic days (E) 12.5 and 13.5 due to cardiovascular defects (Brannan et al. 1994; Jacks et al. 1994). In addition, studies done by knocking out *Nf1* in cultured cells and in various model systems have demonstrated altered neurodevelopmental processes (Lakkis et al. 1999; Zhu et al. 2001; Gutmann et al. 1999; Sanchez-Ortiz et al. 2014; Shin et al. 2012; Durkin et al. 2023). However, the lack of a high-resolution spatio-temporal map has limited our ability to pinpoint why some developmental processes or specific cell populations are most vulnerable to *Nf1* loss.

Although there are some reports of NF1 expression in the brain (Daston et al. 1992; Su et al. 2007; Ryu et al. 2019; Zhu et al. 2001; Provenzano et al. 2014), no one has conducted a comprehensive high-resolution mapping of this protein in mammalian brain development. In this study, we present a high-resolution, comprehensive map of NF1 expression in the developing mouse brain. By utilizing *in situ* hybridization and immunohistochemistry (IHC) techniques, we characterize the precise spatio-temporal distribution of NF1 across major brain regions and cell lineages from early embryonic

stages through postnatal maturation. Moreover, we also utilized a publicly available single-nuclei RNAseq (snRNAseq) database of adult mouse brain to map *Nf1* expression in different cell clusters, at a resolution much higher than achievable by only using classical techniques. These results reveal a graded expression pattern of *Nf1,* which was not shown previously.

Results:

NF1 is expressed in different cell lineages of the murine forebrain

Using IHC, we observed broad NF1 expression in different parts of the mouse forebrain, such as the neocortex, hippocampus, choroid plexus, thalamus, and hypothalamus at postnatal days (P)35 and P0 (**Fig. 1A-E**). Similar localization of *Nf1* mRNA was also observed at P35 and P0 using *in situ* hybridization (**Supplementary Fig. S1A-B"**). Specifically, NF1 showed perinuclear expression in the neocortical plate and white matter as well as CA fields and hilus of hippocampus (**Fig. 1F,G,J,K**). In embryonic ages E17.5 and E14.5, NF1 protein expression was also observed along the lateral and third ventricular linings (**Fig. 1D,E,H,I,L,M**). By colabelling with different cell-type-specific telencephalic markers across development, we identified sets of cells that express the NF1 protein (**Fig. 2**). We observed strong perinuclear labelling of NF1 in all excitatory pyramidal neocortical neurons from the peak neurogenic stage at E14.5 till developed cortical stage at P35 (**Fig. 2A-H,K,L,N**). This includes coexpression with markers specific to all mature pyramidal neurons (NeuN), deep layer-specific neurons (Ctip2), and upper layer neurons (Satb2). When checked for colocalization with the progenitors at the neocortical ventricular zone, NF1 was found perinuclearly in the $Sox2^+$ apical progenitors at E17.5 and E14.5, but not in the $Tbr2^+$ intermediate progenitor cells (**Fig. 2I,J,M**). Further, NF1 was strongly expressed in the hippocampal CA1 and CA3 pyramidal neurons and hilar neurons, but did not label any cells in the dentate gyrus (DG), as observed at P35, P0 and E17.5 (**Fig. 2O-W"**). These were determined by colabelling NF1 with NeuN, marking all differentiated neurons of the hippocampus across ages, and Ctip2, prominently marking CA1 and developing DG at E17.5. Even at E14.5, weak NF1 expression was observed in the ventricular zone of cortical hem and hippocampal primordium/anlage (**Fig. 2X-X"**).

We also observed strong NF1 expression in different subtypes of cortical interneurons at P35, colabelling with Parvalbumin and Somatostatin (**Supplementary Fig. S2A-D"**). Interestingly, NF1 was observed to be present only in certain subsets of $Olig2^+$ oligodendrocyte populations in the major axonal tracts of P35 mouse forebrain, namely corpus callosum, hippocampal commissure, and anterior commissure (**Fig. 3A-F"**). This observation may suggest differential function of molecularly distinct subtypes of oligodendrocytes when NF1 levels are disrupted in the brain.

NF1 is expressed in different cell lineages of the murine cerebellum

Unlike the forebrain, a more restricted protein expression profile of NF1 was observed in the murine cerebellum across the developmental timeline (**Fig. 4A-J"**). Particularly, strong perinuclear NF1 expression was observed in mature and migrating Purkinje cells,

colabelling with Calbindin (**Fig. 4E',F',G'; Fig. 5A-D"**). On the other hand, very low or no IHC signal of NF1 was observed at any stage of cerebellar granule cell development, when colabelled with NeuN (**Fig. 5E-H",M,N**). *Nf1* mRNA was also observed in the parts of cerebellum at P35 and P0 using *in situ* hybridization (**Supplementary Fig. S1C-D"**). Intriguingly, NF1 expression was observed throughout the development of the cerebellar neurons, be it in the migratory state or transitory state at the embryonic nuclear transitory zone (NTZ) or later when forming the deep cerebellar nuclei (DCN) located within the white matter (**Fig. 4E",F",G"H", I,I',J,J'**). It was coexpressed with NeuN, marking neurons at the DCN, from P3 to P35 (**Fig. 5I-K"**); NeuN+ cells were not present in the prospective DCN area at P0 (**Fig. 5L-L"**).

At embryonic stages, the cerebellar anlage have distinct proliferative zones, namely rhombic lip and cerebellar ventricular zone (CVZ) (Leto et al. 2016). At early cerebellar development (E12.5), CVZ is further subdivided molecularly into the Purkinje cell-producing zone and the Pax2$^+$ interneuron-producing zone. Later in development, the whole CVZ becomes potent to produce cerebellar interneurons. Perinuclear NF1 expression was observed around Sox2+ nuclei in the apical progenitors of the CVZ at E12.5 and E14.5 (**Fig. 6 A-B-B",D,E-E"**). However, no overlap was observed in rhombic lip-derived Pax6$^+$ cells at E12.5 or E14.5 (**Fig. 6C-C", F-F"**). We also found NF1 to mark differentiated Pax2$^+$ cells that have migrated out of the interneuron-producing side of the CVZ at E14.5 (**Fig. 4 I,I", Supplementary Fig. S3A-B"**). However, NF1 was expressed in only a small subset of Tbr2+ rhombic lip-derived unipolar brush cells at E14.5 (**Supplementary Fig. S3E-E"**).

Finally, similar to forebrain results, NF1 showed an interesting expression pattern in glial lineages of the cerebellum (**Fig. 7A-N"**). At both the cerebellar folium and the DCN region, NF1 showed perinuclear expression in a subset of Olig2$^+$ oligodendrocytes, as observed at P35 and P12 (**Fig. 7A-H"**). The same trend was observed in the subpopulations of Bergmann glia, which are unipolar astrocytes of the cerebellum (**Fig. 7I-N"**).

Taken together, here we report differential expression of NF1 in the mouse brain, specifically in glial populations, along development. This suggests the possibility of alternate regulatory mechanisms that eventually govern brain function.

NF1 is expressed in distinct cell layers of the eye and olfactory bulb

Beyond regular brain regions, NF1 was also found to be expressed in accessory brain regions like the eye and olfactory bulb, both being connected to neurosensation (**Fig. 8A-R"**). Expression of NF1 in the developing eye was substantially strong in lens, retinal pigmented epithelium (RPE), and neuroretina. In the neuroretina, NF1 was expressed

distinctly in the photoreceptor cell layer (PRC), as well as the ganglionic cell layer, having both retinal ganglionic cells and Müller glial cells. Sox2$^+$ zone of E14.5 and E17.5 neuroretina largely did not overlap with the NF1$^+$ layers, apart from the PRCs (**Fig. 8A,C-F"**). With respect to the developing olfactory bulb, NF1 was observed specifically in the mitral cell layer (MCL) of the main olfactory bulb (AOB) and accessory olfactory bulb from P0 to P35 (**Fig. 8G-J**). NF1 overlapped with NeuN in the MCL at P35 and P12 (**Fig. 8K,L,O-P"**). On the other hand, it did not have much overlap with Pax6+ cells at P3 and P0, apart from posterior AOB (**Fig. 8M,N,Q-R"**).

Reanalysis of single nuclei RNAseq data reveals enriched *Nf1* expression in diverse neural cell types

To determine the expression of *Nf1* at higher resolution, we took the help of publicly available single-nuclei RNAseq databases (Mortberg et al. 2023; Kozareva et al. 2021). In the adult mouse cortex, *Nf1* expression was identified in almost all the marked cortical clusters (**Fig. 9A-C**). However, detailed analysis revealed specific enrichment of *Nf1* transcripts in the lineages of cortical interneurons, oligodendrocytes, and excitatory neurons (**Fig. 9D**). Particularly, *Nf1* expression was found to be highest in the oligodendrocyte lineage. Moreover, among different oligodendrocyte clusters, *Nf1* expression was found to be highest in differentiating oligodendrocytes (**Fig. 9D**). Based on our IHC data, all Olig2+ cells in the cortex were not positive for NF1. Hence, we looked at the percentage of cells positive for *Nf1* expression across different cortical clusters (**Fig. 9E**). Interestingly, oligodendrocyte precursor cells (OPCs) and differentiating OPCs show a very high frequency of *Nf1*-expressing cells than mature oligodendrocytes. This data strongly suggests the importance of NF1 in oligodendrocyte development. Besides oligodendrocytes, cortical interneurons and excitatory pyramidal neurons also exhibit higher frequency and expression, corroborating our IHC findings.

We performed a similar analysis on adult cerebellum and found enriched expression of *Nf1* in CVZ-derivatives, such as cerebellar interneurons, Purkinje cells, Bergmann glia, and rhombic lip-derivative unipolar brush cell (**Fig. 9F-H**). Among these clusters, the highest expression was found in the Bergmann glial cells (**Fig. 9I**). In similar lines with the adult cortex, *Nf1* has shown enriched expression in the oligodendrocyte lineage with a higher frequency of *Nf1*-expressing cells in the OPC cluster as compared to mature oligodendrocytes (**Fig. 9H**). The frequency plot also shows that almost all the cells in the Purkinje cell cluster were positive for *Nf1* expression, which aligns with our IHC expression data.

Overall, these reanalysis results not only validated our IHC data but also helped identify *Nf1* expression in some neural cell types, such as differentiating oligodendrocytes, which are difficult to capture using conventional IHCs. Our in-depth analysis also

uncovered the graded expression pattern of *Nf1* across diverse cell types in the murine adult brain. This may suggest the differential role of *Nf1* in these diverse subtypes.

Discussion:

In this comprehensive study, we demonstrate the spatiotemporal expression of Neurofibromin1 (NF1) in the murine brain across embryonic, perinatal, and adult developmental timepoints, using IHC, *in situ* hybridization, and reanalyses of publicly available single-nuclei RNAseq databases. To our knowledge, this is the first report of NF1 expression study, not only at various major regions of the brain, but also along almost the entire span of development. In this study, we made interesting discoveries in identifying molecularly distinct subtypes of certain glial populations in the forebrain and the cerebellum on the basis of the presence or absence of NF1 expression. The reanalyses of the snRNAseq datasets of adult cortex and cerebellum also showed graded expression of NF1 and indicated the presence of transitory cell populations. It is also encouraging that our IHC data and RNAseq dataset reanalyses fully corroborated each other for the diverse cell lineages across brain regions that we studied.

NF1 is a critical regulator of two important signalling pathways, namely RAS-RAF-ERK and PI3K-AKT-MTOR pathways, regulating cell metabolism and growth across organ systems (Báez-Flores et al. 2023). Clinically, mutations in *NF1* have been implicated in brain tumours such as neurofibroma and glioma, which often affect the eye. Patients with *NF1* mutations can also suffer from a spectrum of neurodevelopmental disorders, including hydrocephalus, epilepsy, white matter dysplasia, autism, intellectual delay, and impairment of motor functions (Lakkis et al. 1999; Zhu et al. 2001; Gutmann et al. 1999; Sanchez-Ortiz et al. 2014; Shin et al. 2012; Durkin et al. 2023; Dubovsky et al. 2001; Lolam & Roy 2025). The revelation of such cell lineage-based expression patterns of this protein will provide molecular and cellular clarity while studying the underpinnings of NF1-related brain disorders or even help understand the differential functions of cellular subtypes of the brain. In our study, we found NF1 is expressed in excitatory neurons and inhibitory interneurons in the neocortex and hippocampus. We may predict that loss of NF1 may disturb the excitation-inhibition balance in the brain circuits, leading to either neural hyperexcitation or depression, both having pathological implications. Our data also suggests that abnormal NF1 levels may have a differential impact on populations of differentiating oligodendrocytes, with the potential to disrupt the homeostasis of cell fate specification across subtypes. We can hypothesize that the unequal regulation of distinct populations of oligodendrocytes may play a role in developing a patient-specific spectrum of white matter dysplasia and other related disorders. In the cerebellum, NF1 is expressed in DCN and developing cerebellar neurons throughout the studied time series. Proper functioning of DCN neurons and associated circuits is critical for having regular motor functions. Abnormal expression of NF1 may cause mislocalization or malfunctioning of these neurons, eventually leading to motor deficits, as commonly seen in patients harbouring *NF1* mutations. Similarly, defects in NF1 may affect the Purkinje

cell- and cerebellar interneuron-related miscoordination. We also observed NF1 expression in subsets of Bergmann glia, cerebellar astrocytic cells that coordinate cell-cell communication, support development, and prevent neurological injury (Araujo et al. 2019; De Zeeuw & Hoogland 2015; Buffo & Rossi 2013). Having the knowledge of which subtype is affected in a disease condition may help identify specific therapeutic interventions.

Beyond the major regions of the brain, we report NF1 expression also in specific layers of the developing eye and olfactory bulb. Specifically, NF1 is expressed in the photoreceptor layer of the neuroretina, which is vital for vision. It is also identified in retinal ganglion cells and Müller glial cells. Abnormal regulation of these cells due to *NF1* mutations may be the reason behind the development of NF1-related optic gliomas. Further, it marks the mitral cells of the olfactory bulb, which are projection neurons critical for processing the sense of odours (Davison & Katz 2007). Damage to these cells or abnormal expression of NF1 in these cells can cause varied effects on the system's functioning. Interestingly, NF1 also strongly marks both anterior and posterior parts of the AOB, which are associated with stereotypic reproductive and defensive behaviours, respectively. It may be interesting to check NF1 expression in the amygdala and olfactory circuits across species to find a probable evolutionarily conserved olfaction mechanism associated with NF1.

In a nutshell, this comprehensive atlas of *Nf1* expression during murine brain development can provide a necessary framework for understanding the cellular origins of NF1-associated neurodevelopmental pathologies and tumorogenesis, and for the advancement of targeted therapeutic interventions. We envisage that this study would be beneficial not only for neuroscientists and clinicians, but also for cancer biologists and evolutionary biologists, spreading interest and information across a much wider readership.

Materials and methods:

Key resources table:

Reagent type/ resource	Designation	Reference/ Source	Identifiers
Mouse	FVB/NJ	Gift from Prof Kathleen Millen, Seattle Children's Research Institute, USA	-
Antibody	Anti-Parvalbumin Antibody	Merck	Millipore (Cat # MAB1572, RRID:AB_2174013)
Antibody	Anti-Somatostatin Antibody, clone YC7	Merck	Sigma-Aldrich (Cat # MAB354, RRID: AB_2255365)
Antibody	Calbindin D28K Monoclonal Antibody (5A9)	Thermo Fisher Scientific	Invitrogen (Cat # MA5-47441, RRID:AB_2942423)
Antibody	SOX2 Monoclonal Antibody (20G5)	Thermo Fisher Scientific	Invitrogen (Cat # MA1-014, RRID:AB_2536667)
Antibody	Ki-67 Monoclonal Antibody (SolA15)	Thermo Fisher Scientific	Invitrogen (Cat # 14-5698-82, RRID:AB_10854564)
Antibody	Olig2 (F9R1H) Mouse Monoclonal Antibody	Cell Signaling Technology	CellSignalingTechnology (Cat # 39588)
Antibody	PAX2 Monoclonal Antibody (3C7)	Thermo Fisher Scientific	Invitrogen (Cat # H00005076-M01)
Antibody	PAX6 Monoclonal Antibody (GT9412)	Thermo Fisher Scientific	Invitrogen (Cat # MA5-50298, RRID:AB_3094028)
Antibody	Anti-NeuN Antibody, clone A60	Merck	Sigma-Aldrich (Cat # MAB377, RRID: AB_2298772)
Antibody	ALDH1L1 mouse monoclonal antibody, clone UMAB43	OriGene	Origene (Cat # UM500039, RRID:AB_2629053)
Antibody	Anti-Iba1 goat polyclonal antibody	Abcam	Abcam (Cat # ab5076, RRID:AB_2224402)

Antibody	Custom Rabbit polyclonal antibody against NF1	Neurodevelopment lab, India	
Antibody	Anti-SATB1 + SATB2 antibody [SATBA4B10] - C-terminal	Abcam	Abcam (Cat # ab51502, RRID:AB_882455)
Antibody	Anti-Ctip2 antibody [25B6]	Abcam	Abcam (Cat # ab18465, RRID:AB_2064130)
Antibody	Anti-Tbr1 Antibody	Merck	Millipore (Ca t# AB2261, RRID:AB_10615497)
Antibody	EOMES Monoclonal Antibody (Dan11mag)	Thermo Fisher Scientific	Invitrogen (Cat # 14-4875-82, RRID:AB_11042577)
Antibody	FOXJ1 Monoclonal Antibody (2A5)	Thermo Fisher Scientific	Invitrogen (Cat # 14-9965-82, RRID:AB_1548835)
Antibody	Goat anti-Mouse IgG (H+L) Highly Cross-Adsorbed Secondary Antibody, Alexa Fluor™ 488 -	Thermo Fisher Scientific	Invitrogen (Cat # A-11029, RRID:AB_2534088)
Antibody	Goat anti-Rabbit IgG (H+L) Highly Cross-Adsorbed Secondary Antibody, Alexa Fluor™ 568 -	Thermo Fisher Scientific	Invitrogen (Cat # A-11036, RRID:AB_10563566)
Antibody	Goat anti-Rat IgG (H+L) Cross-Adsorbed Secondary Antibody, Alexa Fluor™ 647	Thermo Fisher Scientific	Invitrogen (Cat # A-21247, RRID:AB_141778)
Antibody	Goat anti-Chicken IgY (H+L) Secondary Antibody, Alexa Fluor™ 568	Thermo Fisher Scientific	Invitrogen (Cat # A-11041, RRID:AB_2534098)
Antibody	Goat anti-Rabbit IgG (H+L) Highly Cross-Adsorbed Secondary Antibody, Alexa Fluor™ 488	Thermo Fisher Scientific	Invitrogen (Cat # A-11034, RRID:AB_2576217)

Antibody	Donkey anti-Goat IgG (H+L) Cross-Adsorbed Secondary Antibody, Alexa Fluor™ 647	Thermo Fisher Scientific	Invitrogen (Cat # A-21447, RRID:AB_2535864)
Commercial assay/Kit	RNAscope™ 2.5 HD Reagent Kit-RED	Biotechne	ACD (Cat # 322350)
Probe	RNAscope™ Negative Control Probe	Biotechne	ACD (Cat # 320751)
Probe	RNAscope™ Positive Control Probe-Mm-Polr2a	Biotechne	ACD (Cat # 312471)
Probe	RNAscope Probe Mm Nf1 C1	Biotechne	ACD (Cat # 417351)
Software, Algorithm	Fiji	PMID: 22743772	
Software, Algorithm	10x Genomics Cell Ranger v10.0.0		Single-cell analyses
Software, Algorithm	Seurat v5	PMID: 37231261	Single-cell analyses

Mice:
For all the experiments FVB/NjJ mouse strain was used. Mice were housed and bred under pathogen-free conditions in the animal facility at Jawaharlal Nehru Centre for Advanced Scientific Research (JNCASR, India). All mice received food and water *ad libitum* and were subjected to a 12-hour light-dark cycle. Noon of the day of vaginal plug was designated as embryonic day 0.5 (E0.5). The day of birth was designated as postnatal day 0 (P0), which usually occurs between E19-20.

Sample preparation:
Brains from postnatal pups were harvested in phosphate buffer saline (PBS), then were fixed in 10% Formalin Solution neutral buffer (10% NBF) for 48-72 hrs for P35 and 2-6 hrs for all embryonic and early postnatal ages, equilibrated in 30% (wt/vol) sucrose made in 1X PBS, and sectioned at 30 µm on a freezing microtome (Leica, Germany). These sections were then processed for *in situ* hybridization or immunohistochemical procedures.

Immunohistochemistry:

Sections were washed thrice in PBS, boiled in 10 mM sodium citrate solution for antigen retrieval, blocked in 10% serum in PBS with 0.1%Triton X-100, and then incubated for 36-48 hrs at 4°C with primary antibodies. The next day, sections were washed thrice in PBS, incubated with appropriate species-specific secondary antibodies conjugated with Alexa 488, 568, or 647 fluorophores (Invitrogen) for 2 hrs at room temperature and then counterstained with 4′,6-diamidino-2-phenylindole (DAPI) to visualize the nuclei. Sections were coverslipped using Fluoromount G mounting medium (Fisher Scientific, USA). Information regarding the antibodies used in this study is listed in the Key Resources table above. Immunohistochemistry experiments were replicated with biologically independent samples (minimum three). All attempts for replication were successful. No outliers were encountered. Each antibody was validated for mouse and application (IHC) by the respective manufacturer, and the data are publicly available. This was also validated by us in our experiments, replicating published/expected expressions in control tissue.

***In situ* hybridization:**
Assays were run using commercially available probes from Advanced Cell Diagnostics (ACD, Biotechne). Manufacturer-recommended protocols were used without modification. Sections were probed using *Nf1* (Cat# 417351) and counterstained with hematoxylin.

Imaging of brain sections:
Imaging of IHC brain sections was done using CellVoyager™ CQ1 Benchtop High-Content Analysis System using CellPathfinder (Yokogawa, Japan), and later processed in ImageJ software (NIH, Bethesda, Maryland, USA). In-situ slides were visualized under an Olympus VS 200 slide scanner brightfield microscope. Apart from minor adjustments of contrast and brightness to the entire image, there was no additional image alteration. Pseudo-colouring was used to highlight the cells of interest. Figures were prepared on Adobe Illustrator.

Reanalyses of single-nuclei transcriptomics datasets:
Using Single Cell Portal (singlecell.broadinstitute.org/single_cell), we conducted a reanalysis of single-nuclei RNAseq data of adult cerebellum (SCP795) and adult cortex (SCP2126), originally reported by (Mortberg et al. 2023) and (Kozareva et al. 2021), respectively. The Seurat object was downloaded from the portal, and downstream analysis was performed using Seurat v5 (Hao et al. 2024). UMAP clusters were annotated to different neural cell type based on their transcriptomic signature. We specifically focused on examining the expression level of *Nf1* across diverse cell types. Subsequently, we generated the graphical plots with the help of ggplot2 package (Wickham 2016).

Author Contributions:

VL and AR contributed to the study conception, study design, data acquisition, data analysis, and interpretation. VL and AR wrote the first draft of the manuscript, reviewed, and approved the final manuscript. AR provided the funding and infrastructural resources.

Acknowledgements:

We thank Prof Kathleen J Millen, Seattle Children's Research Institute, for gifting the FVB mouse line; Varun M. and Shruti Srivastava for technical support during image acquisition and processing.

Funding:

This work was funded by the Ramalingaswami Re-entry Fellowship (BT/RLF/Re-entry/73/2020) from the Department of Biotechnology (DBT), India (AR); the Prime Minister Early Career research Grant (PM-ECRG, ANRF/ECRG/2024/001273/LS) from the Anusandhan National Research Foundation (ANRF), India (AR); Early Career Award from the International Brain Research Organization (IBRO, ECA-8126694738) (AR); and the intramural funding from the Jawaharlal Nehru Centre for Advanced Scientific Research, India (AR).

Ethics

Animal experimentation: All animal experimentation was conducted in accordance with the guidelines laid down by the Institutional Animal Ethics Committees (IAEC) of Jawaharlal Nehru Centre for Advanced Scientific Research, India (protocols AR 002 and AR 003).

Data/resource availability:

All relevant data and details on resources are provided in the article and its supplementary information.

Conflict of interest:

The authors declare that the research was conducted in the absence of any commercial or financial relationships that could be construed as a potential conflict of interest.

Diversity and inclusion statement

Preparation of this document has involved diversity and inclusion practices relevant to both the scientific content of the paper and authorship and attribution.

References:

Albers, A.C. & Gutmann, D.H., 2009. Gliomas in patients with neurofibromatosis type 1. *Expert Review of Neurotherapeutics*, 9(4), pp.535–539. Available at: https://doi.org/10.1586/ern.09.4.

Araujo, A.P.B., Carpi-Santos, R. & Gomes, F.C.A., 2019. The role of astrocytes in the development of the cerebellum. *Cerebellum (London, England)*, 18(6), pp.1017–1035. Available at: https://doi.org/10.1007/s12311-019-01046-0.

Ayasa, L.A. et al., 2024. Glioblastoma multiforme in a patient with neurofibromatosis type 1: a case report and review of literature. *Journal of Surgical Case Reports*, 2024(8), p.rjae517. Available at: https://doi.org/10.1093/jscr/rjae517.

Báez-Flores, J., Rodríguez-Martín, M. & Lacal, J., 2023. The therapeutic potential of neurofibromin signaling pathways and binding partners. *Communications Biology*, 6(1), p.436. Available at: http://dx.doi.org/10.1038/s42003-023-04815-0.

Balestri, P. et al., 2003. Malformations of cortical development in neurofibromatosis type 1. *Neurology*, 61(12), pp.1799–1801. Available at: https://doi.org/10.1212/01.WNL.0000099080.90726.BA.

Brannan, C.I. et al., 1994. Targeted disruption of the neurofibromatosis type-1 gene leads to developmental abnormalities in heart and various neural crest-derived tissues. *Genes & Development*, 8(9), pp.1019–1029. Available at: http://dx.doi.org/10.1101/gad.8.9.1019.

Buffo, A. & Rossi, F., 2013. Origin, lineage and function of cerebellar glia. *Progress in Neurobiology*, 109, pp.42–63. Available at: https://doi.org/10.1016/j.pneurobio.2013.08.001.

Cichowski, K. & Jacks, T., 2001. NF1 tumor suppressor gene function: narrowing the GAP. *Cell*, 104(4), pp.593–604. Available at: http://dx.doi.org/10.1016/s0092-8674(01)00245-8.

Daston, M.M. et al., 1992. The protein product of the neurofibromatosis type 1 gene is expressed at highest abundance in neurons, Schwann cells, and oligodendrocytes. *Neuron*, 8(3), pp.415–428. Available at: https://doi.org/10.1016/0896-6273(92)90270-N.

Davison, I.G. & Katz, L.C., 2007. Sparse and selective odor coding by mitral/tufted neurons in the main olfactory bulb. *The Journal of Neuroscience: The Official Journal of the Society for Neuroscience*, 27(8), pp.2091–2101. Available at: https://doi.org/10.1523/JNEUROSCI.3779-06.2007.

De Zeeuw, C.I. & Hoogland, T.M., 2015. Reappraisal of Bergmann glial cells as modulators of cerebellar circuit function. *Frontiers in Cellular Neuroscience*, 9, p.246. Available at: https://doi.org/10.3389/fncel.2015.00246.

Dubovsky, E.C. et al., 2001. MR imaging of the corpus callosum in pediatric patients with neurofibromatosis type 1. *AJNR. American Journal of Neuroradiology*, 22(1), pp.190–195. Available at: https://www.ncbi.nlm.nih.gov/pubmed/11158908.

Durkin, J. et al., 2023. Neurofibromin 1 regulates early developmental sleep in Drosophila. *Neurobiology of Sleep and Circadian Rhythms*, 15(100101), p.100101. Available at: http://dx.doi.org/10.1016/j.nbscr.2023.100101.

Gutmann, D.H. et al., 1999. Haploinsufficiency for the neurofibromatosis 1 (NF1) tumor suppressor results in increased astrocyte proliferation. *Oncogene*, 18(31), pp.4450–4459. Available at: https://doi.org/10.1038/sj.onc.1202829.

Hao, Y. et al., 2024. Dictionary learning for integrative, multimodal and scalable single-cell analysis. *Nature Biotechnology*, 42(2), pp.293–304. Available at: https://doi.org/10.1038/s41587-023-01767-y.

Hyman, S.L., Shores, A. & North, K.N., 2005. The nature and frequency of cognitive deficits in children with neurofibromatosis type 1. *Neurology*, 65(7), pp.1037–1044. Available at: https://doi.org/10.1212/01.wnl.0000179303.72345.ce.

Jacks, T. et al., 1994. Tumour predisposition in mice heterozygous for a targeted mutation in Nf1. *Nature Genetics*, 7(3), pp.353–361. Available at: https://doi.org/10.1038/ng0794-353.

Karaconji, T. et al., 2019. Neurofibromatosis type 1: Review and update on emerging therapies. *Asia-Pacific Journal of Ophthalmology (Philadelphia, Pa.)*, 8(1), pp.62–72. Available at: http://dx.doi.org/10.22608/APO.2018182.

Kozareva, V. et al., 2021. A transcriptomic atlas of mouse cerebellar cortex comprehensively defines cell types. *Nature*, 598(7879), pp.214–219. Available at: https://doi.org/10.1038/s41586-021-03220-z.

Lakkis, M.M. et al., 1999. Neurofibromin deficiency in mice causes exencephaly and is a modifier for Splotch neural tube defects. *Developmental Biology*, 212(1), pp.80–92. Available at: https://doi.org/10.1006/dbio.1999.9327.

Leto, K. et al., 2016. Consensus paper: Cerebellar development. *Cerebellum (London, England)*, 15(6), pp.789–828. Available at: http://dx.doi.org/10.1007/s12311-015-0724-2.

Lolam, V. & Roy, A., 2025. Developmental mechanisms underlying pediatric epilepsy. *Frontiers in Neurology*, 16, p.1586947. Available at: http://dx.doi.org/10.3389/fneur.2025.1586947.

Lucas, C.-H.G. et al., 2022. Multiplatform molecular analyses refine classification of gliomas arising in patients with neurofibromatosis type 1. *Acta neuropathologica*, 144(4), pp.747–765. Available at: https://doi.org/10.1007/s00401-022-02478-5.

Martin, G.A. et al., 1990. The GAP-related domain of the neurofibromatosis type 1 gene product interacts with ras p21. *Cell*, 63(4), pp.843–849. Available at: http://dx.doi.org/10.1016/0092-8674(90)90150-d.

Mortberg, M.A. et al., 2023. A single-cell map of antisense oligonucleotide activity in the brain. *Nucleic Acids Research*, 51(14), pp.7109–7124. Available at: https://doi.org/10.1093/nar/gkad371.

Nix, J.S., Blakeley, J. & Rodriguez, F.J., 2020. An update on the central nervous system manifestations of neurofibromatosis type 1. *Acta neuropathologica*, 139(4), pp.625–641. Available at: http://dx.doi.org/10.1007/s00401-019-02002-2.

Plasschaert, E. et al., 2015. Prevalence of Autism Spectrum Disorder symptoms in children with neurofibromatosis type 1. *American Journal of Medical Genetics. Part B, Neuropsychiatric Genetics: The Official Publication of the International Society of Psychiatric Genetics*,

168B(1), pp.72–80. Available at: http://dx.doi.org/10.1002/ajmg.b.32280.

Provenzano, G. et al., 2014. Hippocampal dysregulation of neurofibromin-dependent pathways is associated with impaired spatial learning in engrailed 2 knock-out mice. *The Journal of Neuroscience: The Official Journal of the Society for Neuroscience*, 34(40), pp.13281–13288. Available at: http://dx.doi.org/10.1523/JNEUROSCI.2894-13.2014.

Rietman, A.B. et al., 2017. Motor problems in children with neurofibromatosis type 1. *Journal of Neurodevelopmental Disorders*, 9(1), p.19. Available at: http://dx.doi.org/10.1186/s11689-017-9198-5.

Roth, J., Ber, R. & Constantini, S., 2019. Neurofibromatosis type 1-related hydrocephalus: Treatment options and considerations. *World Neurosurgery*, 128, pp.e664–e668. Available at: https://doi.org/10.1016/j.wneu.2019.04.231.

Ryu, H.-H. et al., 2019. Enriched expression of NF1 in inhibitory neurons in both mouse and human brain. *Molecular Brain*, 12(1), p.60. Available at: https://doi.org/10.1186/s13041-019-0481-0.

Sanchez-Ortiz, E. et al., 2014. NF1 regulation of RAS/ERK signaling is required for appropriate granule neuron progenitor expansion and migration in cerebellar development. *Genes & Development*, 28(21), pp.2407–2420. Available at: http://dx.doi.org/10.1101/gad.246603.114.

Shin, J. et al., 2012. Zebrafish neurofibromatosis type 1 genes have redundant functions in tumorigenesis and embryonic development. *Disease Models & Mechanisms*, 5(6), pp.881–894. Available at: http://dx.doi.org/10.1242/dmm.009779.

Sorrentino, U. et al., 2021. Epilepsy in NF1: Epidemiologic, genetic, and clinical features. A monocentric retrospective study in a cohort of 784 patients. *Cancers*, 13(24), p.6336. Available at: http://dx.doi.org/10.3390/cancers13246336.

Su, W. et al., 2007. Mice with GFAP-targeted loss of neurofibromin demonstrate increased axonal MET expression with aging. *Glia*, 55(7), pp.723–733. Available at: http://dx.doi.org/10.1002/glia.20501.

Wickham, H., 2016. Data Analysis. In *Use R!*. Cham: Springer International Publishing, pp. 189–201. Available at: https://doi.org/10.1007/978-3-319-24277-4_9.

Zhu, Y. et al., 2001. Ablation of NF1 function in neurons induces abnormal development of cerebral cortex and reactive gliosis in the brain. *Genes & Development*, 15(7), pp.859–876. Available at: http://dx.doi.org/10.1101/gad.862101.

Figure legends:

Figure 1: NF1 is expressed in mouse forebrain
(A) Schematics showing representative coronal sections of the mouse forebrain at adult and embryonic stages. NF1 protein expression in whole brain (B-E), hippocampus (E-I), and neocortex (J-M) across descending ages P35, P0, E17.5, and E14.5. (B-E) NF1 is expressed in distinct zones of thalamus (t) and hypothalamus (hy) in the diencephalon. Dotted boxes in (B-E) mark insets of parts of telencephalon, namely the neocortex and hippocampus. (F-I) NF1 expression was observed in CA1, CA3, and hilar cells of hippocampus at E17.5, P0, and P35 (h) as well as along the ventricular lining (arrows, G,H). (J-M) NF1 is strongly expressed in all mature pyramidal neurons perinuclearly and in the ventricular/subventricular progenitor zones of neocortex across development. P, posterior; A, anterior; nctx, neocortex; cc, corpus callosum; wm, white matter; 3V, third ventricle; lv, lateral ventricle; cp, choroid plexus; mz, marginal zone; cp, cortical plate; sp, subplate layer; iz, intermediate zone; vz, ventricular zone; svz, subventricular zone; DG, dentate gyrus. Scalebars: 500μm (B-E); 100μm (F-I); 50μm (J-M).

Figure 2: NF1 colocalizes with mature neurons and apical progenitors of forebrain
(A-D'') NF1 colocalizes with mature neuronal marker NeuN in P35 (A-A'') and P0 (C-C'') neocortical plates (cp); insets show colocalizations indicated as yellow in both ages (B-B'', D-D''). (E-H) NF1 was expressed in both deep and upper neocortical layers. Perinuclear NF1 expression surrounded the nuclear expression of transcription factors Ctip2 and Satb2, respectively demarcating deep and upper layers. (I,J) NF1 is present perinuclearly in $Sox2^+$ apical progenitors at the ventricular zone (vz) but not in $Tbr2^+$ intermediate progenitor cells. (K-M) NF1 was expressed in both the developing cortical plate and apical progenitor zone at E14.5. (N) Schematic of adult mouse brain with dashed boxes highlighting insets of neocortical and hippocampal planes used for detailed evaluation. (O-W'') NF1 was expressed predominantly in the CA fields (CA1, CA3) and hilus of P35, P0, and E17.5 hippocampi, but no or low expression was seen in the granular neurons of dentate gyrus (DG) across ages. Hippocampal neuron-dense regions were denoted by NeuN and Ctip2 expression. (X-X'') At E14.5, the dorsal midline of the telencephalon showed NF1 expression in choroid plexus (cp), ventricular lining, and a subset of mature neurons derived from the cortical hem. Little expression was found in the hippocampal primordium (hp) at this stage. nctx, neocortex; wm, white matter; 3V, third ventricle; LV, lateral ventricle; mz, marginal zone; cp, cortical plate; sp, subplate layer; iz, intermediate zone; vz, ventricular zone; svz, subventricular zone; DG, dentate gyrus; h, hippocampus. Scalebars: 100μm (O-O'', R-R'', U-U'', X-X''); 50μm (A-A'', P-Q'', S-T''); 25μm (C-C'', E-1, K-M, V-W''); 12.5μm (D-D'', F,H,J).

Figure 3: NF1 is expressed in subsets of cortical oligodendrocytes
(A-A'') NF1 was expressed in a subset of Olig2$^+$ oligodendrocytes in the main three cortical commissures of P35 mouse brain - corpus callosum (A-B''), anterior commissure (C-D''), and hippocampal commissure (E-F''). In a magnified view, cream dashed circles mark NF1$^+$Olig2$^+$ double-positive oligodendrocytes, while red dotted circles mark Olig2$^+$ oligodendrocytes that did not express NF1 (B-B", D-D", F-F"). Scalebars: 50μm (A-A'', C-C'', E-E''); 25μm (B-B'', D-D'', F-F'').

Figure 4: NF1 is expressed in the mouse cerebellum
(A-D) Schematics showing sagittal sections of the mouse forebrain at adult, early postnatal, and embryonic stages, demonstrating how a complex lobular laminated structure like the cerebellum develops from a simple fate-specified neuroepithelium. Boxes mark insets at P35, P12, P3 and P0 indicating magnified views of folium and cerebellar ventricular zone. (E-F'') P35 and P12 cerebella showed strong NF1 expression in the Purkinje cell layer (pcl), cells in the white matter (wm), and in the deep cerebellar nuclei (DCN). (G-H'') NF1 was also expressed in migrating Purkinje cells and in developing DCN at perinatal ages P3 and P0. (I-J"") At E14.5 and E12.5, NF1 was expressed very strongly in immature cerebellar neurons of the nuclear transitory zone (NTZ), and in differentiating neurons near the cerebellar ventricular zone (cvz) and/or extra cerebellar ventricular zone. NF1 was also expressed at weaker levels in migrating rhombic lip-derived cells. NF1 was expressed in the hindbrain choroid plexus (cp) across the developmental stages, from E12.5 to the adult stage. Mes, mesencephalon; rl, rhombic lip; ml, molecular layer; gcl, granular cell layer; egl, external granular cell layer; igl, internal granular cell layer. Scalebars: 200μm (E,F,G,H,I,J); 50μm (E'-F"); 20μm (G'-H", I'-J'').

Figure 5: NF1 is expressed in cerebellar neuronal lineages across development
(A-D") NF1 was expressed in Purkinje cells across development, and arrowheads show its colocalization with Calbindin (Calb). Insets show magnified views of one Calb$^+$ Purkinje cell across development and its colocalization with NF1. (E-H") Colabelling NF1 with NeuN marking cerebellar granule cells showed no or low coexpression across development. (I-L") NF1 expression was predominant in the mature neurons of deep cerebellar nuclei (DCN) across development, colocalizing with NeuN (cream dashed circles). NeuN$^+$ mature cells were not observed here at P0. (M,N) Schematics demonstrate morphology and differential lamination of developing (<P21) and developed (>P21) mouse cerebella. Mes, mesencephalon; rl, rhombic lip; ml, molecular layer; gcl, granular cell layer; egl, external granular cell layer; igl, internal granular cell layer; bv, blood vessels; cp, choroid plexus; bg, Bergmann glia. Scalebars: 25μm (A-B", E-F"); 10μm (C-D", G-L").

Figure 6: NF1 is expressed in the embryonic cerebellar ventricular progenitors
(A,D) Schematics demarcate different germinal zones of cerebellar anlage at E14.5 and E12.5. At E12.5, the cerebellar ventricular zone is subdivided into the zone producing Purkinje cells (deep blue) and the interneuron-producing zone (light blue). (B-B", E-E") NF1 is expressed perinuclearly in Sox2+ progenitors in the cerebellar ventricular zone at E12.5 and E14.5. However, NF1 was not expressed in Pax6+ secondary progenitor cells derived from the rhombic lip. Mes, mesencephalon; NTZ, nuclear transitory zone. Scalebars: 20μm (B-F").

Figure 7: NF1 is expressed in cerebellar glial lineages
(A-H") NF1 was expressed in a subset of Olig2$^+$ oligodendrocytes in both folium (A-D") and deep cerebellar nuclei (E-H") at mature (P35) and developing (P12) mouse cerebella (arrowheads). In magnified views (B-B",D-D",F-F",H-H"), cream dashed circles mark NF1$^+$Olig2$^+$ double-positive oligodendrocytes, while red dotted circles mark Olig2$^+$ oligodendrocytes that did not express NF1. (I-N") NF1 was also expressed in the soma and projection of the Bergmann glia across development. Colocalization with Blbp is shown using arrowheads. ml, molecular layer; gcl, granular cell layer; egl, external granular cell layer; igl, internal granular cell layer; pcl, Purkinje cell layer; wm, white matter. Scalebars: 25μm (A-A", C-C", E-E", G-G", I-I", K-K", M-M"); 10μm (B-B", D-D", F-F", H-H", J-J", L-L", N-N").

Figure 8: Nf1 expression in murine optic cup and olfactory bulb
(A,B) Schematics showing zones and cell layers of neurosensory organs, eye and olfactory bulb. (C,F") NF1 is expressed in the developing mouse eye, predominantly in the lens (L) and neuroretina (NR) at E17.5 and E14.5. Magnified insets (D-D", F-F") show coexpression of NF1 protein with the photoreceptor layer (PRC, arrowheads) and retinal ganglionic cells and Müller glial cells in the broad ganglionic cell layer (GC). NF1 showed wide coexpression with Sox2 in PRC and retinal pigmented epithelium (RPE). (G-J) NF1 was expressed strongly across the postnatal development of the olfactory bulb. It showed strong expression in the mitral cell layer (MCL) of the main olfactory bulb (MOB) and also in the accessory olfactory bulb (AOB). (K,L,O-P") Colabelling with NeuN at P35 and P12 identified subsets of mitral cells that were double positive for NF1 and NeuN (arrowheads). (M,N, Q-R") Strong coexpression with Pax6 was seen in posterior AOB (pAOB) at P0 and P3, but not in the other parts of MOB. IN, interneurons; aAOB, anterior accessory olfactory bulb; EPL, external plexiform layer; GCL, granule cell layer; GL, glomerular layer. Scalebars: 200μm (G,H,K,L); 100μm (C-C", E-E", I,J,M,N); 50μm (O-O", P-P"); 25μm (Q-R"); 20μm (D-D", F-F").

Figure 9: Reanalysis of single nuclei RNAseq data showing expression of *Nf1* in adult mouse brain

(A**,**F) UMAP plot for single nuclei RNAseq data from adult mouse cortex and cerebellum, respectively. Transcriptionally distinct clusters were coloured based on cell type. (B,G) UMAP plot illustrating the expression level of *Nf1* (red) across different cortical and cerebellar clusters, respectively. (C-E) *Nf1* expression is higher in cortical interneurons, differentiating OPCs, and excitatory neurons of adult murine cortex compared to other neural populations. (H-J) In adult murine cerebellum, *Nf1* expression is enriched primarily in Purkinje cells, Golgi INs, Bergmann glia, and OPCs. MGE_INs, medial ganglionic eminence interneurons; dMGE_INs, dorsal medial ganglionic eminence interneurons; CGE_INs, caudal ganglionic eminence interneurons; OPCs, oligodendrocyte precursor cells; MLI, molecular layer interneurons; PLI, Purkinje layer interneurons; INs, interneurons; UBC, unipolar brush cells.

FIGURES

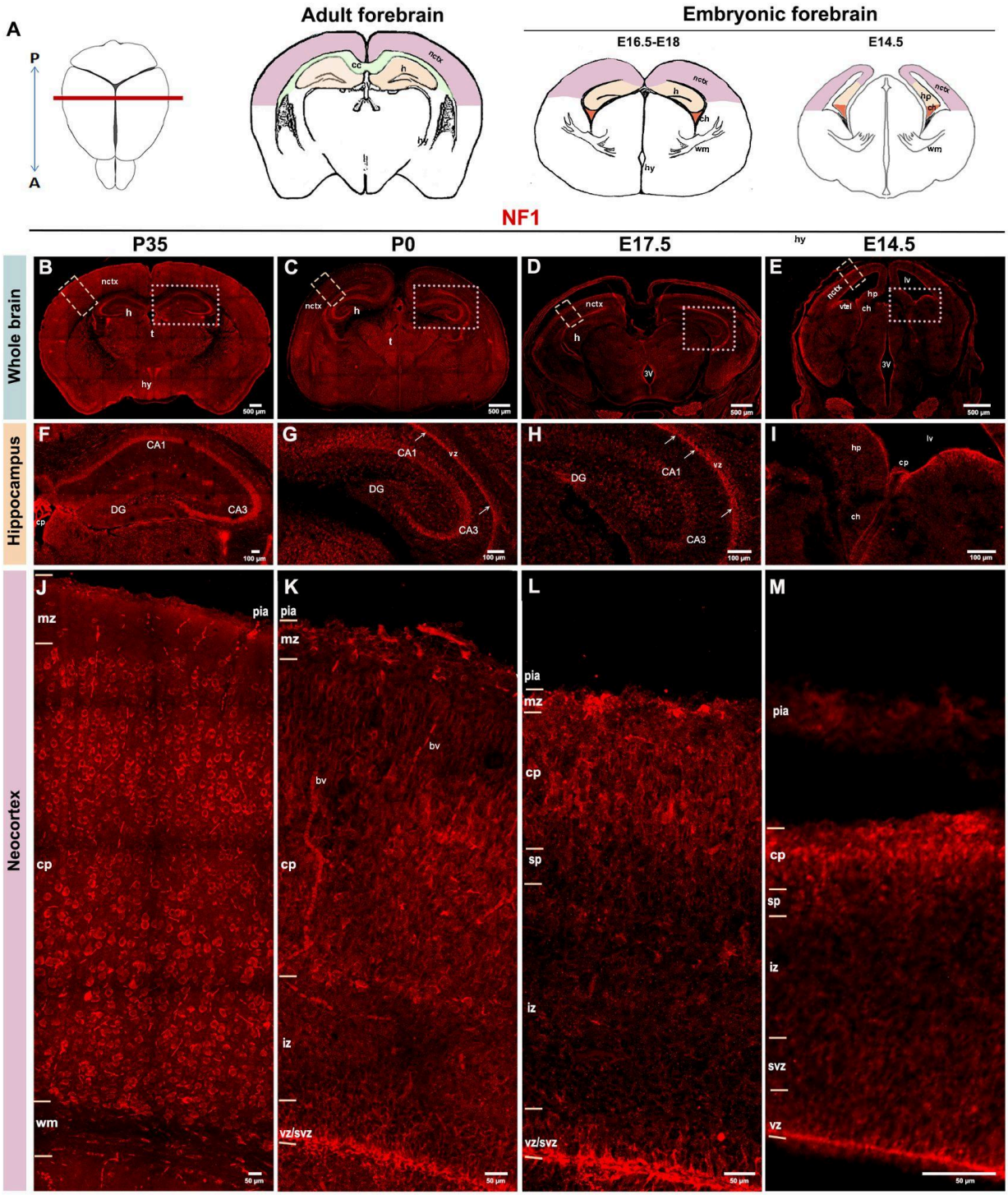

Figure 1

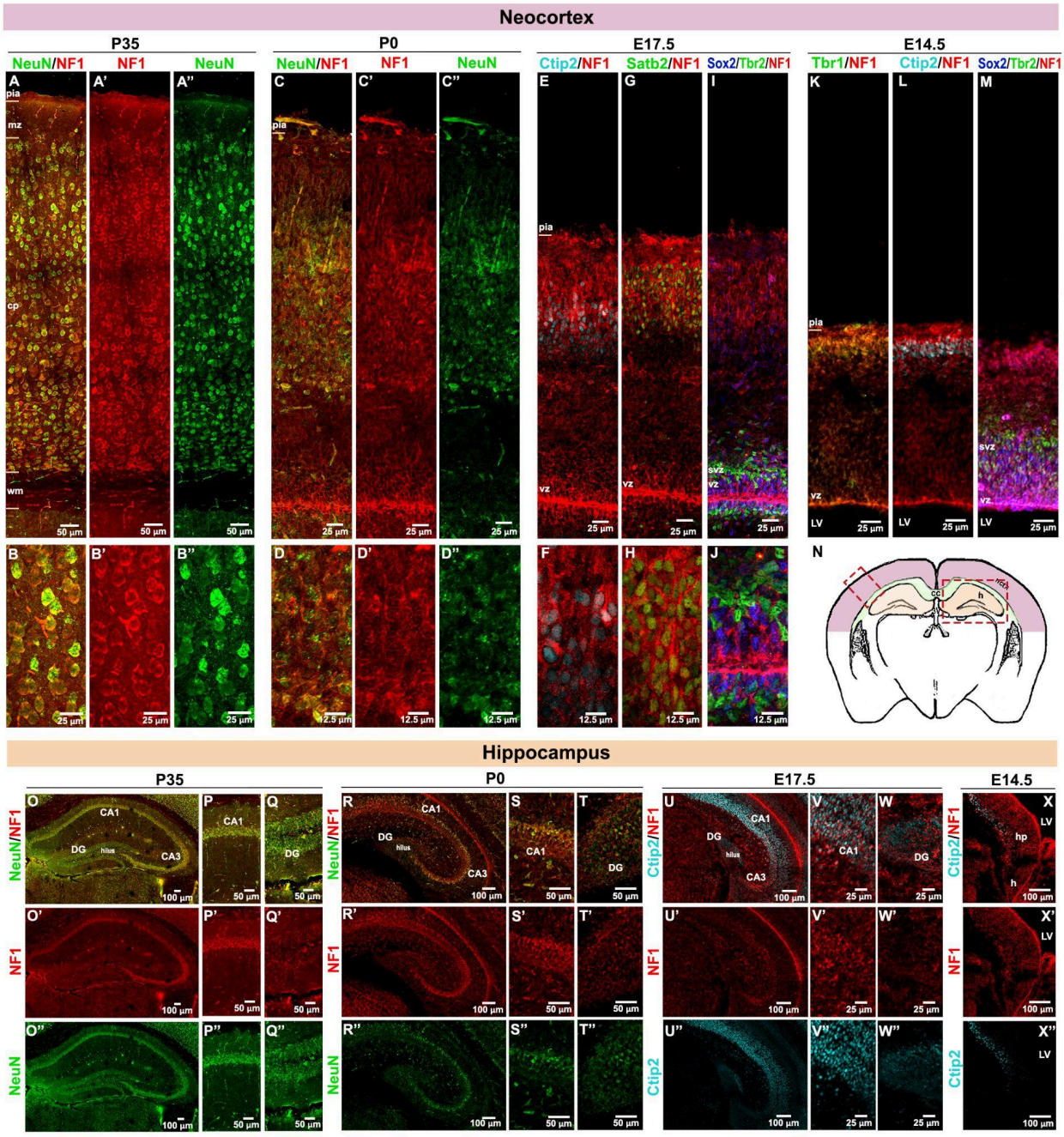
Neocortex
P35
P0
E17.5
E14.5
NeuN/NF1
NF1
NeuN
Ctip2/NF1
Satb2/NF1
Sox2/Tbr2/NF1
Tbr1/NF1
pia
mz
cp
wm
vz
svz
LV
Hippocampus
CA1
DG
hilus
CA3
hp
h

Figure 2

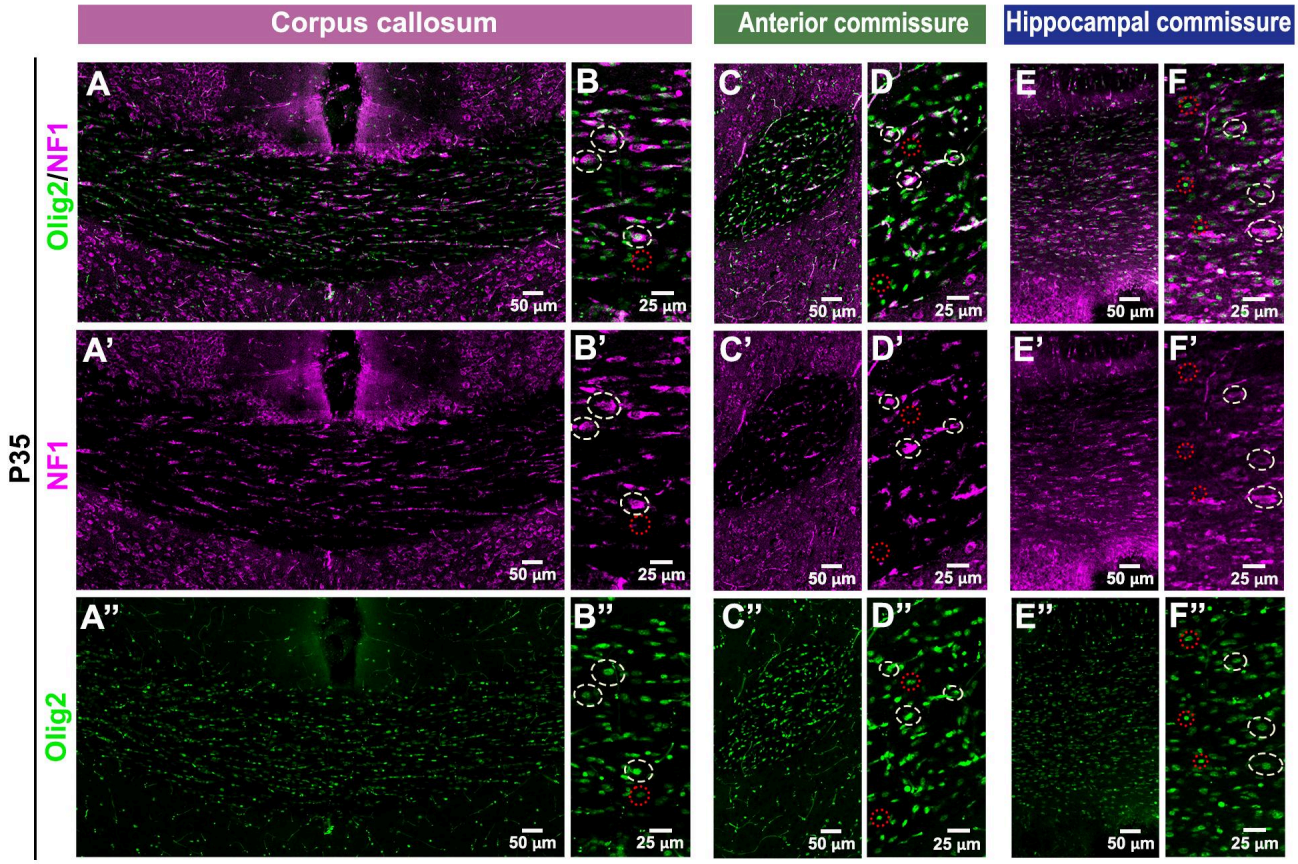
Corpus callosum
Anterior commissure
Hippocampal commissure
P35
Olig2/NF1
NF1
Olig2
A
B
C
D
E
F
A'
B'
C'
D'
E'
F'
A''
B''
C''
D''
E''
F''
50 µm
25 µm

Figure 3

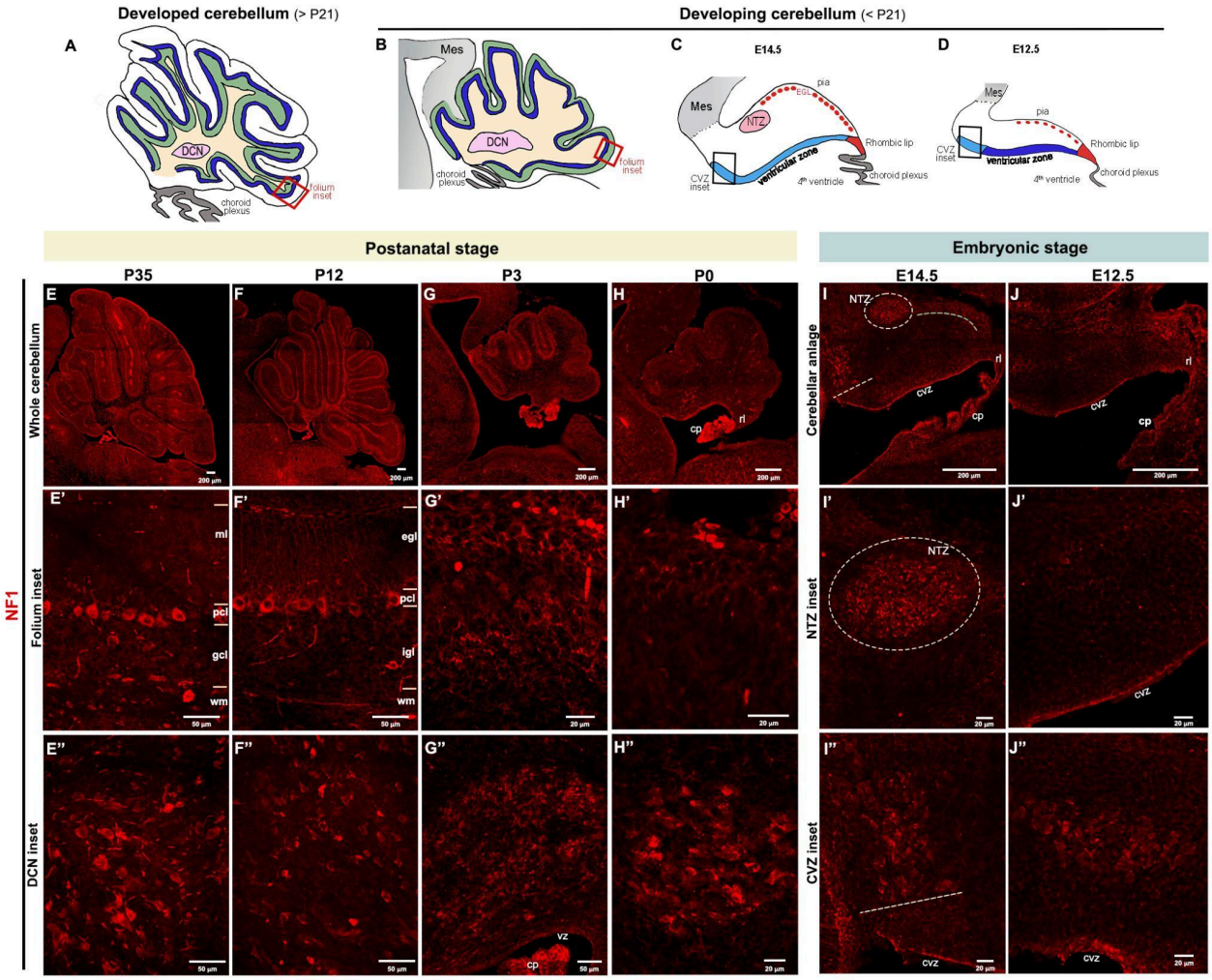
Developed cerebellum (> P21)
Developing cerebellum (< P21)
A
B
C
D
E14.5
E12.5
Mes
DCN
NTZ
pia
Rhombic lip
ventricular zone
CVZ inset
4th ventricle
choroid plexus
folium inset
Postanatal stage
Embryonic stage
P35
P12
P3
P0
E14.5
E12.5
Whole cerebellum
Folium inset
DCN inset
Cerebellar anlage
NTZ inset
CVZ inset
NF1
ml
pcl
gcl
wm
egl
igl
rl
cp
cvz
vz
200 µm
50 µm
20 µm

Figure 4

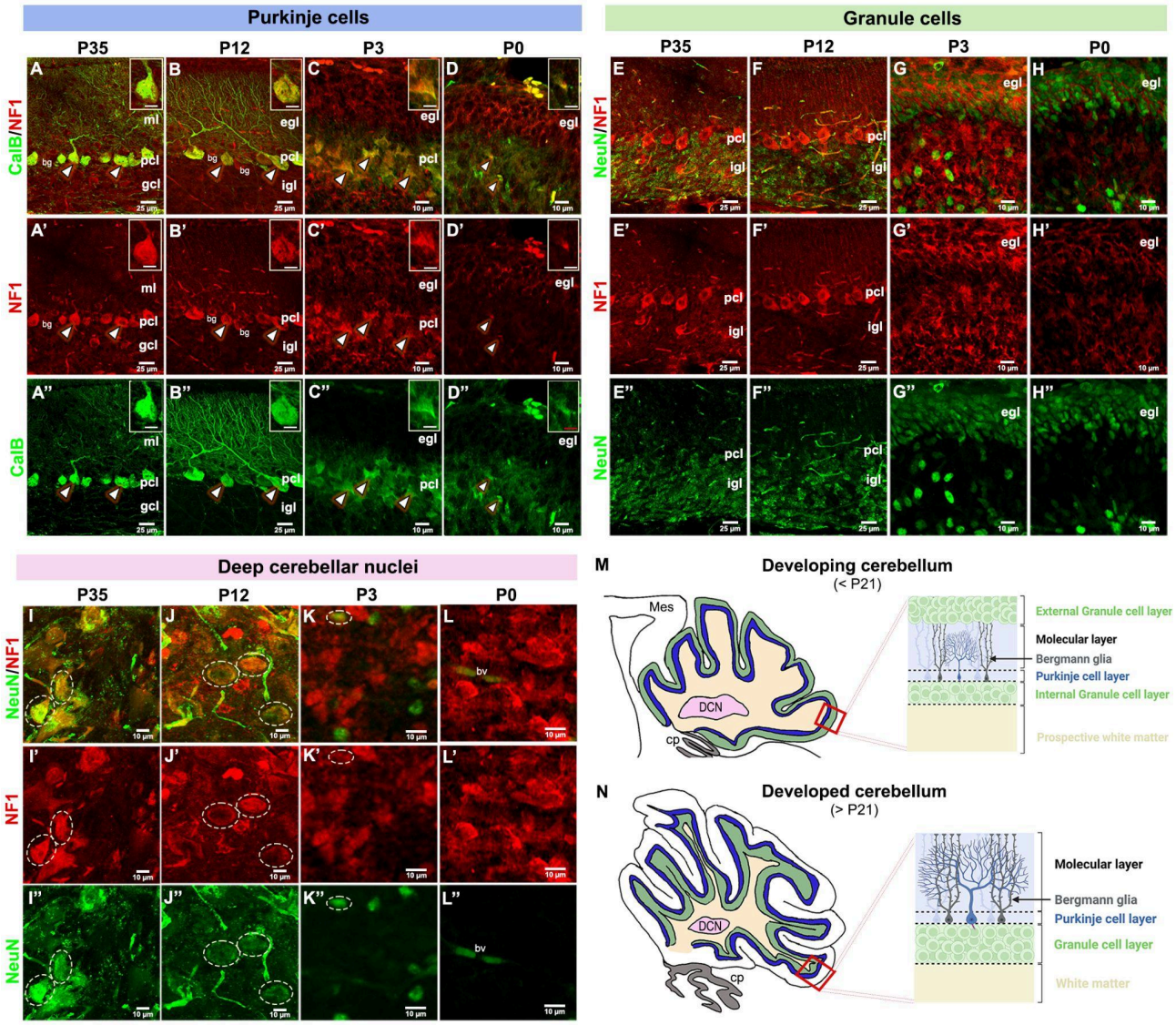
Purkinje cells
Granule cells
P35
P12
P3
P0
CalB/NF1
NF1
CalB
NeuN/NF1
NeuN
ml
pcl
gcl
igl
egl
bg
Deep cerebellar nuclei
bv
M
Developing cerebellum
(< P21)
Mes
DCN
cp
External Granule cell layer
Molecular layer
Bergmann glia
Purkinje cell layer
Internal Granule cell layer
Prospective white matter
N
Developed cerebellum
(> P21)
Molecular layer
Bergmann glia
Purkinje cell layer
Granule cell layer
White matter

Figure 5

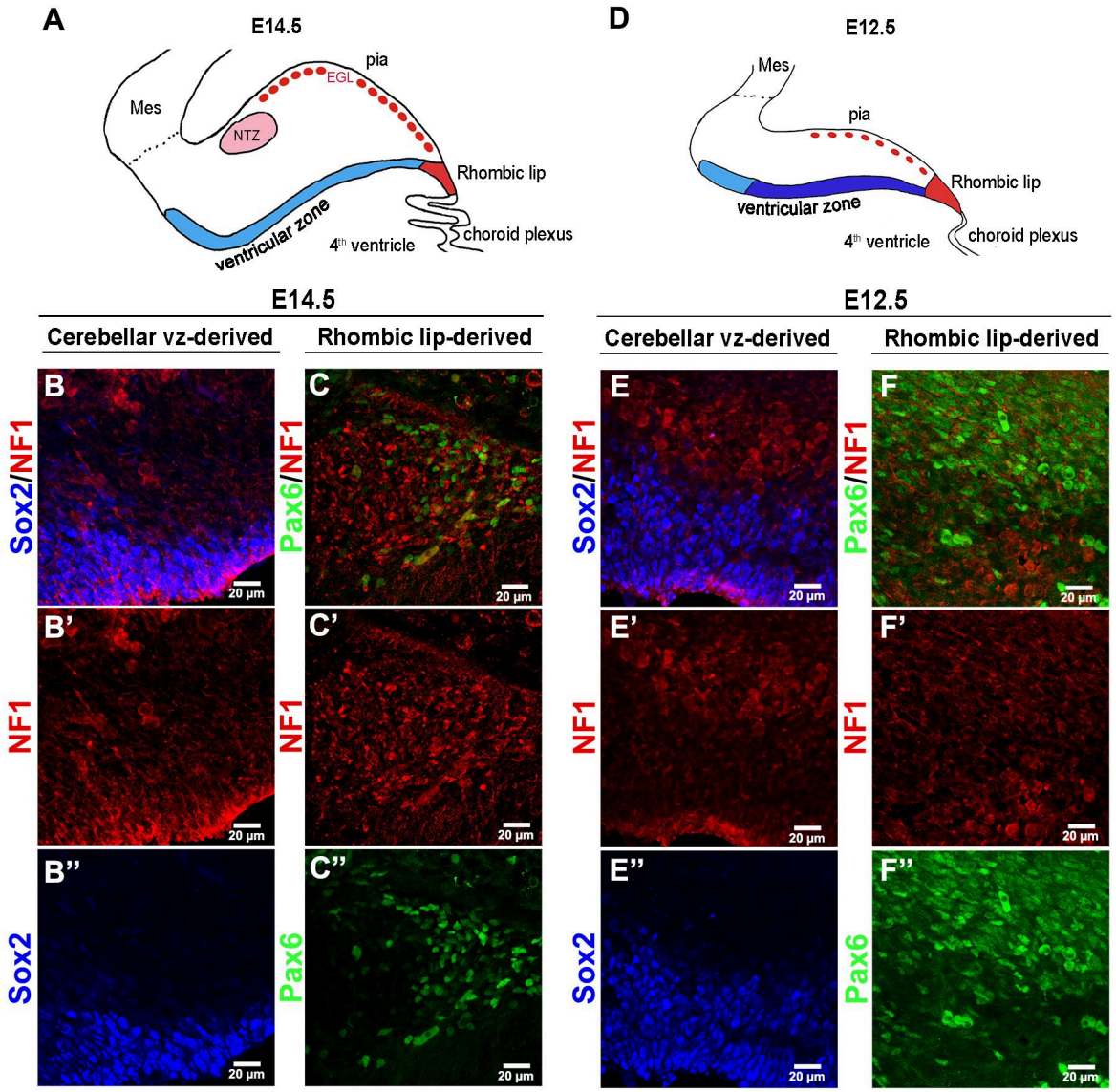
A
E14.5
pia
EGL
Mes
NTZ
Rhombic lip
ventricular zone
4th ventricle
choroid plexus
D
E12.5
Mes
pia
Rhombic lip
ventricular zone
4th ventricle
choroid plexus
E14.5
Cerebellar vz-derived
Rhombic lip-derived
E12.5
Cerebellar vz-derived
Rhombic lip-derived
Sox2/NF1
Pax6/NF1
NF1
Sox2
Pax6
B
C
E
F
B'
C'
E'
F'
B''
C''
E''
F''
20 µm

Figure 6

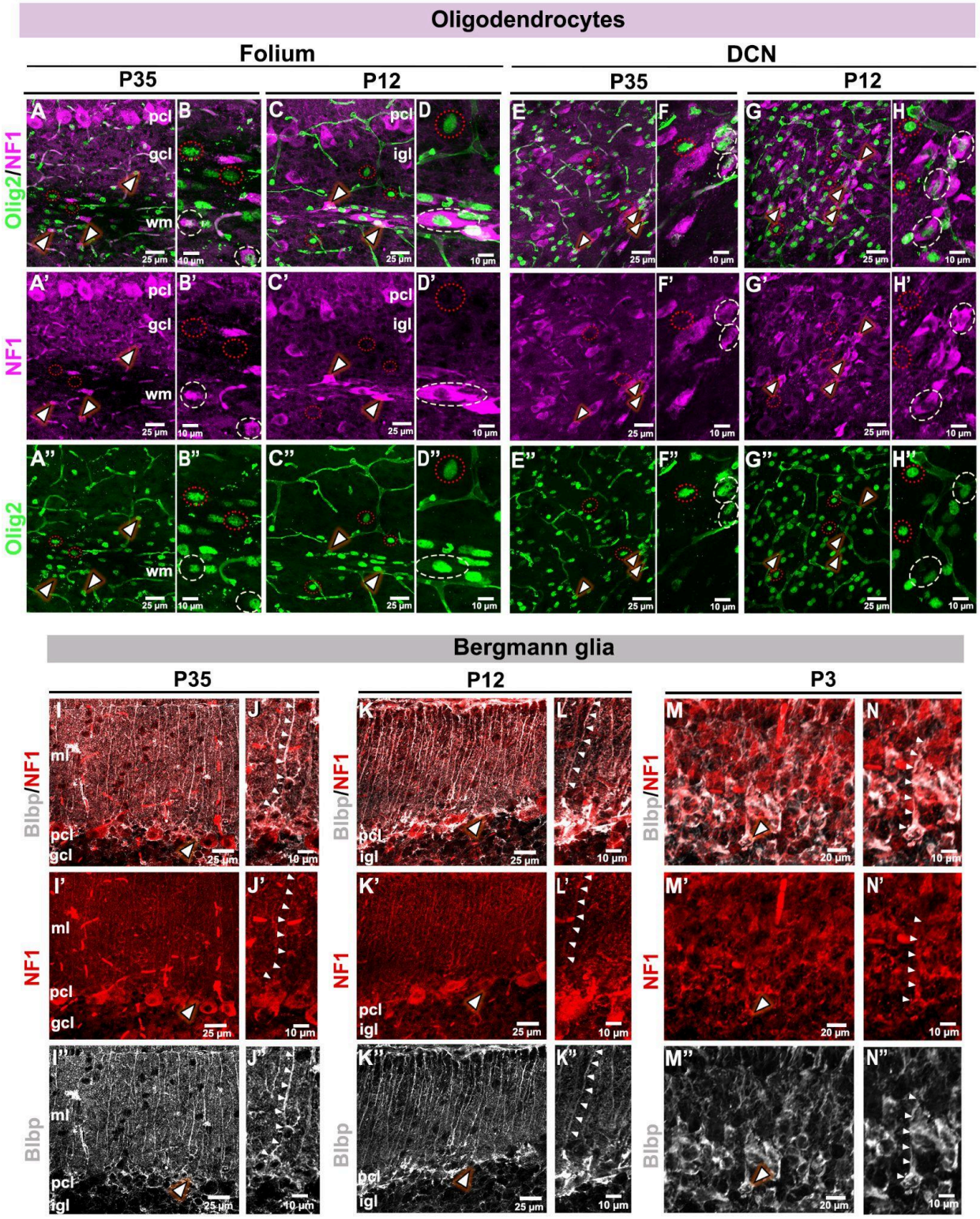
Oligodendrocytes
Folium
DCN
P35
P12
P35
P12
Olig2/NF1
NF1
Olig2
pcl
gcl
wm
igl
25 µm
10 µm
Bergmann glia
P35
P12
P3
Blbp/NF1
NF1
Blbp
ml
pcl
gcl
igl
20 µm

Figure 7

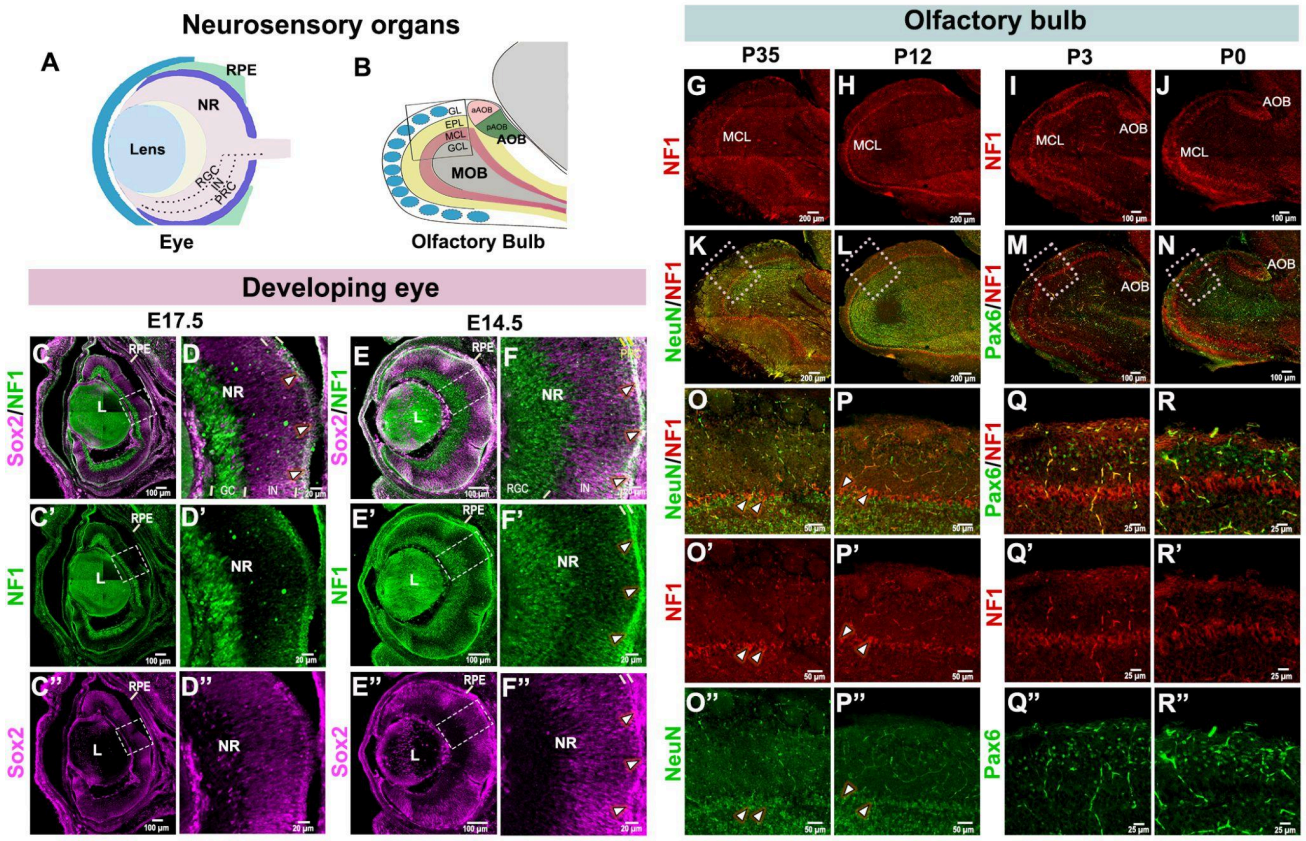
Neurosensory organs
A
RPE
NR
Lens
RGC
IN
PRC
Eye
B
GL
EPL
MCL
GCL
aAOB
pAOB
AOB
MOB
Olfactory Bulb
Developing eye
E17.5
E14.5
Sox2/NF1
NF1
Sox2
RPE
L
NR
GC
IN
RGC
Olfactory bulb
P35
P12
P3
P0
MCL
AOB
NeuN/NF1
Pax6/NF1
NeuN
Pax6

Figure 8

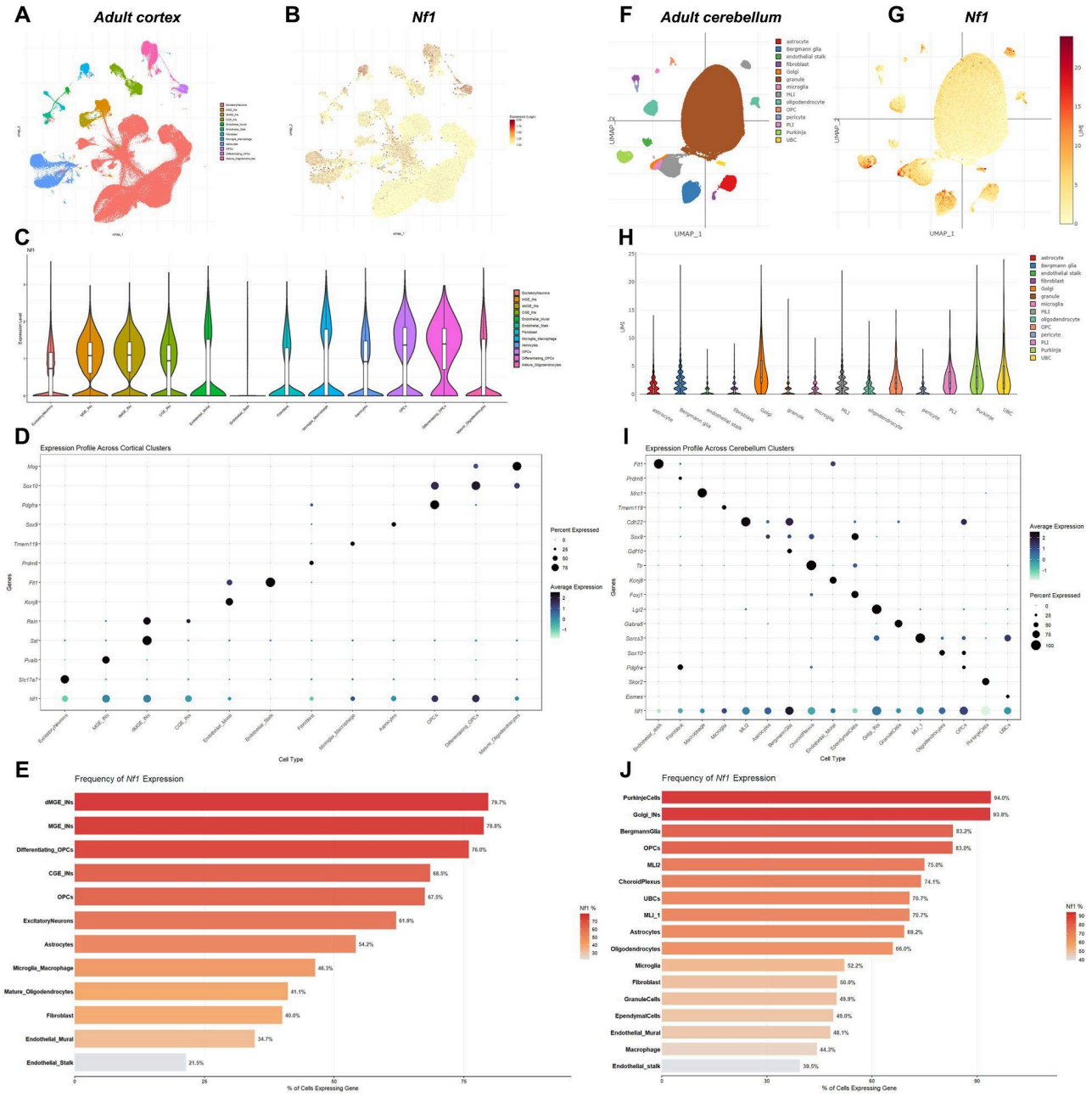
A
Adult cortex
B
Nf1
F
Adult cerebellum
G
Nf1
C
D
Expression Profile Across Cortical Clusters
Percent Expressed
Average Expression
Genes
Cell Type
E
Frequency of Nf1 Expression
dMGE_INs 79.7%
MGE_INs 78.8%
Differentiating_OPCs 76.0%
CGE_INs 68.5%
OPCs 67.5%
ExcitatoryNeurons 61.9%
Astrocytes 54.2%
Microglia_Macrophage 46.3%
Mature_Oligodendrocytes 41.1%
Fibroblast 40.0%
Endothelial_Mural 34.7%
Endothelial_Stalk 21.5%
Nf1 %
% of Cells Expressing Gene
H
I
Expression Profile Across Cerebellum Clusters
J
Frequency of Nf1 Expression
PurkinjeCells 94.0%
Golgi_INs 93.8%
BergmannGlia 83.3%
OPCs 83.0%
MLI2 75.0%
ChoroidPlexus 74.1%
UBCs 70.7%
MLI_1 70.7%
Astrocytes 69.2%
Oligodendrocytes 66.0%
Microglia 52.2%
Fibroblast 50.0%
GranuleCells 49.9%
EpendymalCells 49.0%
Endothelial_Mural 48.1%
Macrophage 44.3%
Endothelial_stalk 39.5%

Figure 9